A Methodology for Two-dimensional Finite Element Analysis of Electromagnetically Driven Flow in Induction Stirring Systems

Thinium T. Natarajan
US Steel Technical Center, Monroeville, PA 15146

Nagy El-Kaddah
The University of Alabama, Tuscaloosa, AL 35487

***Abstract*—This paper describes an integral closure approach for 2-D analysis of electromagnetically driven flow in inductively coupled molten metal using the finite-element method. This methodology, which restricts the solution domain to the conducting regions(s), was demonstrated for flows generated by complex electromagnetic fields, and computed results were found to be in good agreement with measurements.**

***Index Terms*— Eddy currents, fluid flow, modeling, numerical methods.**

I. Introduction

Induction technologies are extensively used for stirring of molten metal by means of electromagnetic forces generated from the interaction between induced currents in the melt and the associated magnetic field. The range of applications extends from scrap melting in induction furnaces to melt stirring in continuous casting [1]. With the increased use metallic shields to modify the force distribution in the melt and hence the flow, modeling has become an indispensable tool for the analysis of electromagnetically driven flows in these applications. The problem with the conventional differential approach for describing the electromagnetic field in eddy current problems is the expansion of the solution domain to infinity. This renders the numerical solution of the coupled electromagnetic and fluid flow equations using finite element or finite difference methods to be computationally inefficient.

The hybrid differential-integral approach, which eliminates the solution of the magnetic field in free space, provides a practical framework for the analysis of electromagnetically driven flow in induction stirring systems [2,3]. An alternative to the finite element-boundary integral method is the integral closure method proposed by the authors for the numerical solution of the field in the conducting region [4,5]. It is based on the specification of the magnetic field boundary condition on the outer surface of the conductor using the Biot-Savart law.

Manuscript received June 1, 1998

T. T. Natarajan, 412-825-2088, Fax 412-825-2800, ttnatarajan@uss.com; N. El-Kaddah, 205-348-1743, Fax 205-348-2164, nelkaddah@coe.eng.ua.edu.

The purpose of this paper is to extend this methodology to complex induction systems comprised of multi-conductor domains and to present an integrated finite element methodology for modeling electromagnetic and fluid flow phenomena in induction furnaces.

II. Governing Electromagnetic And Flow Equations

Consider a liquid metal in a cylindrical or rectangular container surrounded by metallic rings and an induction coil as shown in Fig. 1. The passage of alternating current, I, in the coil generates a 2-d magnetic field, $\mathbf{B}$ $(B_1, 0, B_3)$. The current in conducting regions has only one component in the x_2 direction. For a time-harmonic applied field with angular frequency ω, the electromagnetic field in the conducting domains $(\Omega_1,..,\Omega_{nc})$ may be represented in terms of the vector potential, $\mathbf{A}$ $(0, A_2, 0)$, by:

$$\nabla^2 A_{2,j} = c\frac{A_{2,j}}{h_2^2} + j\sigma\mu_0\omega A_{2,j} \qquad \forall\ j = 1..n_c \tag{1}$$

where μ_o the is magnetic permeability, σ is the electrical conductivity of the conductor, j is $\sqrt{-1}$, h_3 is the coordinates' scale factor, and c is constant equal to 0 for cartesian coordinates, and 1 for cylindrical coordinates.

In order to use this equation to compute the field in the system without solving for the field in free space, one needs to know A on boundaries of conducting domains. In this methodology, the boundary conditions for A are supplied by Biot-Savart law, which may be expressed as:

$$A_{s,j} = \frac{\mu_0}{4\pi}\left(\sum_{turns} I\oint\frac{dl}{|\mathbf{r}-\mathbf{r}'|} + \sum_{i=1}^{n_c}\int_{\Omega^i}\frac{j\sigma\omega A}{|\mathbf{r}-\mathbf{r}'|}dV^i\right) \tag{2}$$

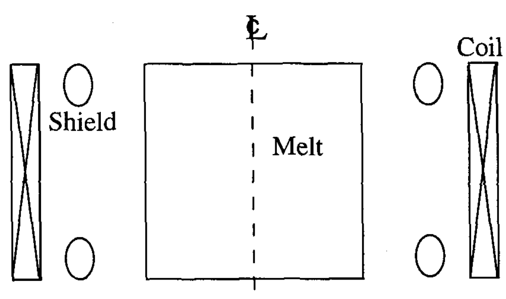

Fig. 1. Sketch of the System

The force field resulting from JXB in the liquid metal, which is in the x_1 and x_3 directions, generates a two-dimensional velocity field, $\mathbf{U}(u_1,0,u_3)$. For steady flow, the time-averaged continuity and turbulent Navier-Stokes equations for u_1 and u_3 are:

$$\nabla.\mathbf{U} = -\frac{p}{\lambda} \tag{3}$$

$$\rho((U\cdot\nabla)u_1) = -\frac{\partial p}{\partial x_1} + \mu_{eff}\left(\nabla^2 u_1 + c\cdot\frac{u_1}{h_2^2}\right) + \frac{1}{2}Re(J_2 B_3^*) \tag{4}$$

$$\rho((U\cdot\nabla)u_3) = -\frac{\partial p}{\partial x_3} + \mu_{eff}(\nabla^2 u_3) - \frac{1}{2}Re(J_2 B_1^*) \tag{5}$$

where ρ is the density, μ_{eff} is the effective viscosity, p is pressure and λ is the penalty parameter [6]. Using the k-ε turbulent model [7], μ_{eff} is:

$$\mu_{eff} = \mu_l + \rho C_\mu k^2/\varepsilon \tag{6}$$

where μ_l is the molecular viscosity of the fluid, k is the turbulent kinetic energy, ε is the turbulent energy dissipation.

The boundary conditions needed to solve (3)-(6) are zero velocity at solid walls and zero velocity gradients at the melt free surface and at the axis or plane of symmetry.

III. Finite Element Formulation

In this work, the finite element formulation of the electromagnetic field problem was developed using the Bubnov-Galerkin method, while the fluid flow equations were discretized using Petrov-Galerkin method.

From the weak integral form of (1), the global finite element matrix equation of the field problem for any conducting domain may be expressed as:

$$\left[\sum_{j=1}^{N}([K_1]+c[K_2]+[K_3])\right]\cdot\{A_3\} = 0 \tag{7}$$

$$[K_1] = \int_{\Omega_j}(\nabla N^T\cdot\nabla N)dV, \qquad [K_2] = \int_{\Omega_j}\frac{N^T N}{h_3^2},$$

$$[K_3] = j\sigma\omega\mu_0\int_{\Omega_j}N^T N\,dV$$

where N is the shape function. The value of A at the nodes on the boundaries of the conducting region are specified by (2).

Upon manipulating the weak forms of (3) to (5), the final matrix equation of the fluid velocities may be written as:

$$\begin{bmatrix} K_{11}+\lambda C_1 C_1^T & \lambda C_1 C_3^T \\ \lambda C_3 C_1^T & K_{33}+\lambda C_3 C_3^T \end{bmatrix}\cdot\begin{Bmatrix} u_1^{n+1} \\ u_3^{n+1} \end{Bmatrix} = \begin{Bmatrix} F_1 + C_1 P^n \\ F_3 + C_3 P^n \end{Bmatrix} \tag{8}$$

$$K_{ii} = \int_\Omega\left[(W^T(U\cdot\nabla)N) + \nabla W^T\cdot\nabla N\right]dV$$

$$C_i = \int_\Omega\frac{\partial W^T}{\partial x_i}dV,\ C_i^T = \int_\Omega\frac{\partial N^{\prime T}}{\partial x_i}\cdot dV,\ W = N + \frac{\alpha h}{2\cdot|u|}(u\cdot\nabla)N$$

$$P^{n+1} = P^n + \lambda[C]^T\{u\} \tag{9}$$

where W is the weight function, |u| is the magnitude of velocity vector, and parameter α is defined in [6]. The superscript n denotes the iteration number.

IV. Solution Technique

The developed formulation allows the treatment of each conducting region as a separate domain from meshing, assembly and solution of the matrix equations standpoints. This approach not only reduces the size of the field stiffness matrix, but also facilitates combining the fluid flow and electromagnetic field algorithms. The solution of the governing equations essentially involves the calculation of the electromagnetic field in the conducting domains followed by the calculation of the electromagnetic forces and flow in the molten metal region.

The algorithm for computing the electromagnetic field begins with the solution of (7) using an estimated A on the boundaries of the conducting regions from the coil current. This step is repeated with updated A from the previous solution until an identical solution is obtained. The convergence criterion for error definition R_E was 10^{-3}.

$$R_E = \left[\frac{\sum(\phi^{i+1}-\phi^i)^2}{\sum(\phi^i)^2}\right] \tag{10}$$

In computing the Lorentz force (J X B) at the nodal points of the fluid domain B was evaluated from the Biot-Savart law. In this work, four-point Gaussian quadrature was used to evaluate the integral of J in this equation.

The fluid flow algorithm involves the solution of the velocity matrix equation (8), followed by updating the pressure field and turbulent viscosity fields using (9) and (6), respectively. This procedure is repeated till the error between two successive iterations using the error definition in (10) is less than 10^{-3}. For the cases examined, it took between 100-130 iterations to obtain converged velocity solution.

V. Application To Induction Furnaces

The developed solution methodology was applied to simulate electromagnetically driven flow in a mercury physical model of the induction furnace [8]. Two cases were examined. The first deals with stirring in absence of metallic shields, while the second involves field modification using copper rings for the configuration shown in Fig. 1. The geometrical and electrical data are summarized in Table I. All calculations were carried out using 725 quadrilateral elements in the liquid, and 121 elements in the copper ring.

TABLE I
INPUT DATA USED IN THE CALCULATIONS

Inner radius of the container	0.075 m
Height of mercury in the container	0.2 m
Radius of the copper ring	0.0875 m
Major and minor axis of the shield	0.018, 0.013 m
Radius of the induction coil	0.15 m
Number of coil turns	303
RMS coil current	32.51 Amps
Frequency	50 Hz
Electrical conductivity of mercury	10^6 mho/m
Electrical conductivity of copper	6 10^7 mho/m

Fig. 2a and 2b shows the computed magnetic field streamlines with and without field modification. These figures show that the induced field in the melt distorts the applied magnetic field, and the distortion is more pronounced near the outer surface of the molten region. Inspection of these figures indicates that the effect of the shield is to further distort the magnetic flux lines.

Fig. 3 to 5 shows a comparison between computed and measured axial profiles of the magnetic field and induced currents in the liquid mercury for the two cases. Quantitative agreement is seen regarding the numerical values of these field quantities within experimental errors. It is also seen that the measured and computed profiles are quite similar, and the model predicts reasonably well the distortion of the magnetic field the shields.

Fig. 6 and 7 shows the axial and radial variation of Fz, which is the principal driving force of the flow. Again, the agreement is seen to be very good between the measurements and predictions. This together with the ability to resolve the reversal of the force direction by the shields with relatively few elements demonstrates the viability of the present method for the analysis of the flow in induction stirring systems.

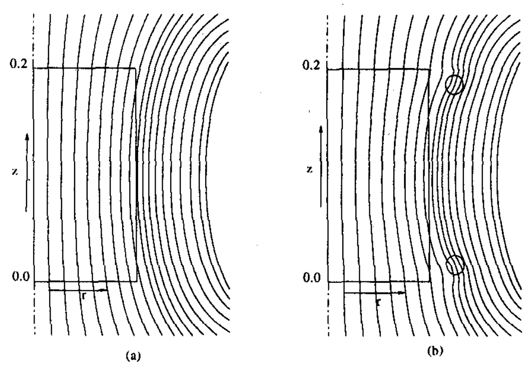

Fig. 2. Computed magnetic streamlines: (a) without shields, (b) with shields.

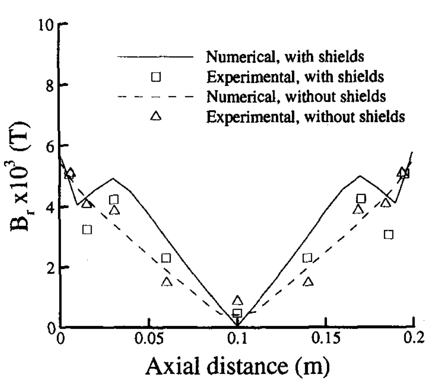

Fig. 3. Measured and predicted axial variation B_r at r=0.07 m.

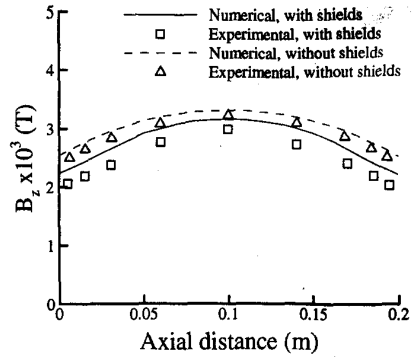

Fig. 4 Measured and predicted axial variation of B_z at r=0.07 m.

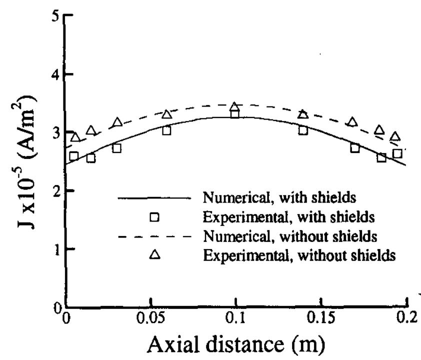

Fig. 5. Measured and predicted axial variation of J at r=0.07 m.

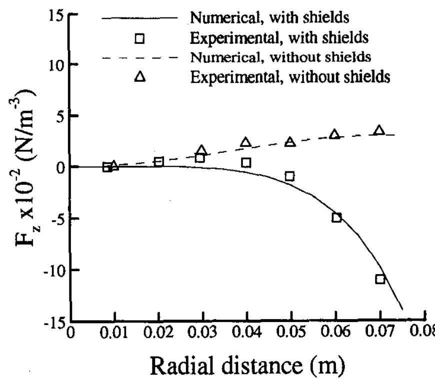

Fig. 6. Measured and predicted radial variation of F_z at z=0.17 m.

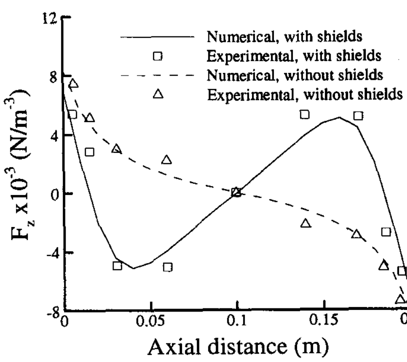

Fig. 7. Measured and predicted axial variation of F_z at r=0.07 m.

Figs. 8a and 8b show the effect of the metallic shield in modifying the flow. These figures clearly show that the presence of the shields significantly modifies the flow pattern from two recirculating loops to four recirculating loops. Furthermore, it alters the direction of the flow in these loops. The reversal of the flow is clearly shown in Fig. 9, which shows the radial variation of the velocity at the axial position corresponding to the eye of the vortex. The agreement between the computed and measured velocities regarding both the direction and magnitude for these two cases not only validates the model formulation. Also, it demonstrates the robustness of the model in resolving the electromagnetic and velocity fields with fewer elements.

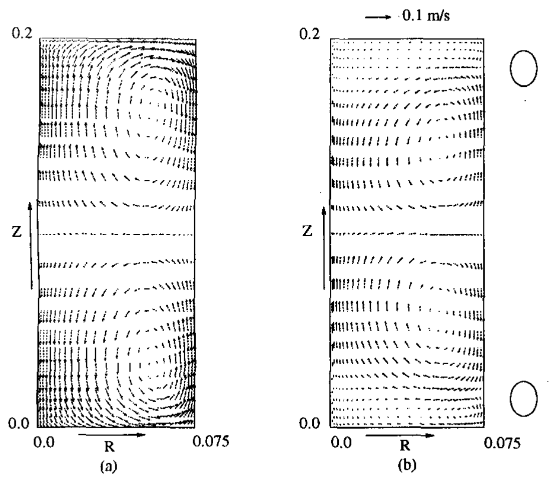

Fig. 8. Plot of velocity vectors in an induction furnace: (a) without shields, and (b) with shields.

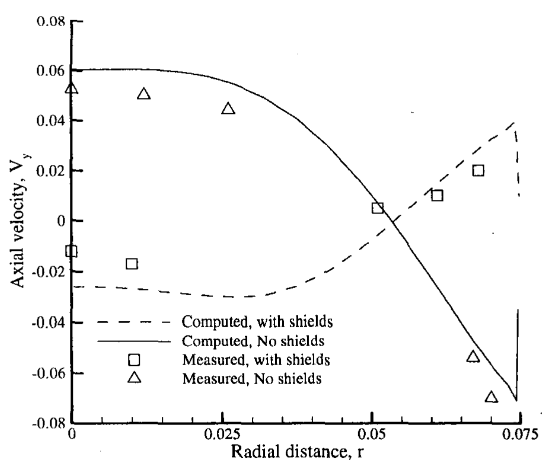

Figure 9 Comparison between measured and predicted radial variation of V_z at r=0.07 m.

VI. Concluding Remarks

A finite element based computational approach has been described for the simultaneous solution of the electromagnetic and fluid flow equations in 2-D induction stirring systems. The key to this computational technique, which limits the solution domain to the conduction region, is the integral description of the electromagnetic field boundary condition for closure of the differential field equation. This alternative formulation to the hybrid FEM-BIM method is easier to implement specially for systems with many discrete conducting regions. Through the decomposition and solution of the field in small domains as well as the calculation of the flow in the molten region only, the developed method offers considerable savings in memory and CPU time requirements. Finally, the robustness of this method has been demonstrated by accurately predicting the measured electromagnetic parameters and melt velocities in a physical model of induction furnace with a relatively small number of elements.

References

[1] Garnier, M., "Magnetohydrodynamics in Material Processing," *Phil. Trans. R. Soc. London.* A (1993), pp.249-263.

[2] Salon, S. J., and Schneider, J. M., "A Hybrid Finite Element-Boundary element Formulation of the Eddy Current Problem," *IEEE Trans. on Magnetics*, vol. 18(2), 1982, pp. 461-466.

[3] Gyimesi, M., Tsukerman, I., Laver, D., Pawlak, T., and Ostergard, D., "Hybrid Finite Element-Treffetz Method for Open Boundary Analysis," *IEEE Trans. on Magnetics*, vol. 32(3), (1996), pp. 671-674.

[4] Meyer, J. L., El-Kaddah, N., and Szekely, J., "A New Method for Computing Electromagnetic Force Fields in Induction Furnaces," *IEEE Trans. on Magnetics*, vol. 23(2), 1987, 1806-1810.

[5] Natarajan, T. T., and El-Kaddah, N., "A Finite Element-Integral Method for Two-Dimensional Eddy Current Problems," *Proceedings of TMS Symposium on Magnetohydrodynamics in Process metallurgy*, Eds. J. Szekely et. al., TMS, (1991), pp. 3-9.

[6] Zienkiewicz, O. C., and Taylor, R. L., *The Finite Element Method*, vol. 2, McGraw Hill, London, (1991).

[7] Launder, B. E., and Spalding, D. B., *Lectures in Mathematical Models of Turbulence*, Academic Press, London, Second Edition, (1972).

[8] Vives, C. and Ricou, R., "Fluid Flow Phenomena in a Single Phase Coreless Induction Furnace," *Met Trans. B*, vol. 16B, (1985), pp. 227.